NeuroImage: Clinical 4 (2014) 130–138

Contents lists available at ScienceDirect

NeuroImage: Clinical

journal homepage: www.elsevier.com/locate/ynicl

Multiple sclerosis impairs regional functional connectivity in the cerebellum ☆

Anne-Marie Dogonowski [a,*,1], Kasper Winther Andersen [a,d,1], Kristoffer Hougaard Madsen [a,d], Per Soelberg Sørensen [b], Olaf Bjarne Paulson [a,c], Morten Blinkenberg [b], Hartwig Roman Siebner [a]

[a] Danish Research Centre for Magnetic Resonance, Centre for Functional and Diagnostic Imaging and Research, Copenhagen University Hospital Hvidovre, Kettegaard Allé 30, 2650 Hvidovre, Denmark
[b] Danish Multiple Sclerosis Center, Department of Neurology, Copenhagen University Hospital Rigshospitalet, Blegdamsvej 9, 2100 København Ø, Denmark
[c] Neurobiology Research Unit, Copenhagen University Hospital Rigshospitalet, Juliane Maries Vej 24, Building 9201, 2100 København Ø, Denmark
[d] Cognitive Systems, Department of Applied Mathematics and Computer Science, Technical University of Denmark, Matematiktorvet, Building 321, 2800 Lyngby, Denmark

ARTICLE INFO

Article history:
Received 3 June 2013
Received in revised form 14 November 2013
Accepted 15 November 2013
Available online 27 November 2013

Keywords:
Cerebellum
fMRI
Multiple sclerosis
Regional connectivity
Resting-state

ABSTRACT

Resting-state functional magnetic resonance imaging (rs-fMRI) has been used to study changes in long-range functional brain connectivity in multiple sclerosis (MS). Yet little is known about how MS affects functional brain connectivity at the local level. Here we studied 42 patients with MS and 30 matched healthy controls with whole-brain rs-fMRI at 3 T to examine local functional connectivity. Using the Kendall's Coefficient of Concordance, regional homogeneity of blood-oxygen-level-dependent (BOLD)-signal fluctuations was calculated for each voxel and used as a measure of local connectivity. Patients with MS showed a decrease in regional homogeneity in the upper left cerebellar hemisphere in lobules V and VI relative to healthy controls. Similar trend changes in regional homogeneity were present in the right cerebellar hemisphere. The results indicate a disintegration of regional processing in the cerebellum in MS. This might be caused by a functional disruption of cortico-ponto-cerebellar and spino-cerebellar inputs, since patients with higher lesion load in the left cerebellar peduncles showed a stronger reduction in cerebellar homogeneity. In patients, two clusters in the left posterior cerebellum expressed a reduction in regional homogeneity with increasing global disability as reflected by the Expanded Disability Status Scale (EDSS) score or higher ataxia scores. The two clusters were mainly located in Crus I and extended into Crus II and the dentate nucleus but with little spatial overlap. These findings suggest a link between impaired regional integration in the cerebellum and general disability and ataxia.

1. Introduction

Multiple sclerosis (MS) is characterised by disseminated inflammatory demyelination and axonal degeneration in the central nervous system. The disease-related tissue damage delays and disrupts neural signal transmission along cortico-cortical and cortico-subcortical connections (Trapp et al., 1998), causing inefficient information transfer between brain regions. Accordingly, functional magnetic resonance imaging (fMRI) of spontaneous fluctuations in the blood-oxygen-level-dependent (BOLD)-signal during the resting-state has demonstrated changes in long-range functional connectivity of MS patients in the motor network (Dogonowski et al., 2012; Lowe et al., 2002; Roosendaal et al., 2010) and the default-mode network (Hawellek et al., 2011; Rocca et al., 2010).

In addition to studying long-range connectivity within functional brain networks, resting-state fMRI (rs-fMRI) can also be used to assess local connectivity in a brain region. The homogeneity of resting-state BOLD-signal fluctuations in neighbouring voxels reflects local brain connectivity (Zang et al., 2004). Regional homogeneity has successfully been used to identify abnormal local connectivity in pathological conditions such as neuromyelitis optica, Alzheimer's and Parkinson's disease (He et al., 2007; Liang et al., 2011; Wu et al., 2009). Here we employed regional homogeneity analysis of resting-state BOLD-signal fluctuations to test for brain regions where MS patients express an abnormal pattern of local functional connectivity relative to healthy controls. Within the patient group, we were also interested to identify brain regions where the regional expression of local resting-state connectivity would predict clinical disability.

* Corresponding author at: Danish Research Centre for Magnetic Resonance, Copenhagen University Hospital Hvidovre, Department 340, 2650 Hvidovre, Denmark. Tel.: +45 3862 3331; fax: +45 3647 0302.
E-mail addresses: annemd@drcmr.dk (A.-M. Dogonowski), kwjo@dtu.dk (K.W. Andersen), stoffer@drcmr.dk (K.H. Madsen), per.soelberg.soerensen@rh.regionh.dk (P.S. Sørensen), olaf.paulson@nru.dk (O.B. Paulson), blink@dadlnet.dk (M. Blinkenberg), h.siebner@drcmr.dk (H.R. Siebner).
[1] These authors contributed equally to the manuscript.

2213-1582/$ – see front matter © 2013 The Authors. Published by Elsevier Inc. All rights reserved.
http://dx.doi.org/10.1016/j.nicl.2013.11.005

2. Subjects and methods

2.1. Patients and healthy subjects

Forty-two patients with definite MS fulfilling the revised McDonald criteria (Polman et al., 2005) and 30 sex- and age-matched healthy controls participated in the study. 39 of the 42 patients and 27 of the 30 healthy controls were right-handed as revealed by the Edinburgh Inventory (Table 1) (Oldfield, 1971). Healthy subjects had no history of neurological or psychiatric disease. The study was approved by the scientific ethics committee of Copenhagen and Frederiksberg Communities (protocol no. KF01—131/03 with addendum) and all subjects gave written informed consent.

Patients were recruited from The Danish Multiple Sclerosis Center, Copenhagen, Denmark and comprised 27 patients with relapsing–remitting MS (RR-MS) and 15 patients with secondary progressive MS (SP-MS) (Table 1). Only clinically stable patients who had not experienced a relapse in the three months preceding the magnetic resonance imaging (MRI) measurement were included. Neurological or psychiatric symptoms not attributable to MS were defined as exclusion criteria. Patients were neurologically examined and clinical disability was rated using the Expanded Disability Status Scale (EDSS) (Kurtzke, 1983). The EDSS score ranges from 0 to 10 where 0 equals a normal neurological examination and higher scores indicate more disability. In our patient group, EDSS scores ranged from 0–7 (median score: 4.3). The degree of ataxia was rated using the Multiple Sclerosis Impairment Scale (Ravnborg et al., 1997). The ataxia score evaluated upper and lower limb ataxia and ranges from 0 to 16, where 0 equals no ataxia and the highest scores correspond to the inability to perform coordinated movements. The individual ataxia scores ranged from 0–13 (median score: 3). 81% of the patients (n = 34) presented with ataxia defined as having an ataxia score above 0.

2.2. Magnetic resonance imaging

MRI measurements were performed on a 3 T Magnetom Trio scanner. All rs-fMRI measurements were recorded with a standard single-channel birdcage head-coil using a T2*-weighted echo planar imaging (EPI) sequence with a repetition time (TR) of 2490 ms, an echo time (TE) of 30 ms and a flip angle of 90°. In total 480 whole-brain volumes were acquired over 20 min. A brain volume consisted of 42 contiguous axial slices with a slice thickness of 3 mm and a 64 × 64 acquisition matrix covering a field of view = 192 × 192 mm. The resulting voxel size was 3 × 3 × 3 mm. Subjects were instructed to rest with their eyes closed without falling asleep, and refrain from any voluntary cognitive or motor activity. After the experiment, participants were asked whether they managed to stay awake. All participants reported that they did not fall asleep during scanning. The cardiac cycle was monitored with an infrared pulse oximeter attached to the index finger. Respiration was monitored with a pneumatic thoracic belt. Participants refrained from caffeine, cigarettes or alcohol intake six hours prior to the fMRI-session. Patients continued to take their usual medication.

Additionally, high-resolution three-dimensional structural MRI scans of the brain were acquired using an eight-channel phased array coil (Invivo, FL, USA). A sagittal magnetisation prepared rapid acquisition gradient echo (MPRAGE) sequence (TR = 1550 ms, TE = 3.04, inversion time = 800 ms; flip-angle = 9°) was acquired consisting of 192 contiguous slices with a voxel size of 1 × 1 × 1 mm and an acquisition matrix of 256 × 256. In addition, sagittal turbo spin echo (TSE) images (TR = 3000 ms, TE = 354 ms) and fluid-attenuated inversion recovery (FLAIR) images (TR = 6000 ms, TE = 353 ms) were obtained. The TSE and FLAIR images covered the whole brain consisting of 192 slices with a voxel size of 1.1 × 1.1 × 1.1 mm and a 256 × 256 acquisition matrix. The structural scans were used to estimate total lesion load of cerebral white-matter in MS patients and to exclude subclinical white-matter lesions in healthy controls. Whole-brain lesion load was quantified using a semi-automatic lesion segmentation method guided by expert knowledge as described previously (Dogonowski et al., 2012).

Patients with MS showed reduced regional homogeneity in the cerebellum. This prompted us to perform a follow-up analysis on the patient data in which we tested for a linear relationship between lesion load in the cerebellar peduncles and the cortico-spinal tract (CST) and the change in regional homogeneity in the cerebellum. Lesion load in the cerebellar peduncles was estimated by extracting the cerebellar peduncles including the inferior, middle, and superior cerebellar peduncles as defined in the JHU white-matter tractography atlas and split into a left and right region-of-interest (ROI) (Hua et al., 2008). Lesion load of the inferior, middle, and superior cerebellar peduncles was also estimated individually. The ROI applied to estimate lesion load of the left, right and combined CST was specified as defined in JHU white-matter tractography atlas (Hua et al., 2008).

Table 1
Demographics and clinical characteristics.

	Healthy controls	Patients with MS	RR-MS	SP-MS
Number of subjects	30	42	27	15
(men; women)	(15; 15)	(20; 22)	(10; 17)	(10; 5)
Median age in years	45	45	39	51
(range)	(22–69)	(25–64)	(25–59)	(30–64)
Handedness	27; 2; 1	39; 3; 0	26; 1; 0	13; 2; 0
right; left; ambidextrous				
Median disease duration in years	n.a.	11.5	9	20
(range)		(3–43)	(3–27)	(6–43)
Median EDSS score	n.a.	4.3	3.5	6.0
(range)		(0–7)	(0–6.5)	(3.5–7.0)
Median ataxia score	n.a.	3.0	2.0	4.0
(range)		(0–13)	(0–13)	(1–10)
Median whole-brain lesion load in ml	n.a.	21.4 (n = 41)	17.4 (n = 26)	35.8 (n = 15)
(range)		(1.8–126.3)	(1.8–96.6)	(3.7–126.3)
Median lesion load in left and right cerebellar peduncles in ml	n.a.	0.04	0.05	0.04
(range)		(0–1.1)	(0–1.1)	(0–0.8)
Treatment	n.a.	35	24	11
IFN-β	n.a.	6	6	0
Glatiramer acetate	n.a.	9	9	0
Natalizumab	n.a.	5	5	0
Immunosuppresive agents	n.a.	10	5	5
Other	n.a.	6	0	6

MS = multiple sclerosis; RR-MS = relapsing–remitting multiple sclerosis; SP-MS = secondary progressive multiple sclerosis; n.a. = not applicable; EDSS = Expanded Disability Status Scale; IFN = Interferone.

2.3. Resting-state fMRI data analysis

2.3.1. Pre-processing

Image pre-processing of the EPI images used statistical parametric mapping (SPM) software (SPM8, Wellcome Trust Centre for Neuroimaging, http://www.fil.ion.ucl.ac.uk/spm) implemented in Matlab 7.9 (MathWorks, Massachusetts, USA). The first five brain volumes were discarded to account for T1 equilibrium effects. The remaining 475 brain volumes were first realigned to the first volume in the time series, then a mean volume was generated, and the realignment procedure was repeated with this volume as the target. The volumes were then co-registered to the same-session T1-weighted MPRAGE data set using a six-parameter rigid-body transformation. The MPRAGE volumes were spatially normalised to the Montreal Neurological Institute (MNI) 305 standard template using the unified segmentation and normalisation procedure as implemented in SPM8 and the same normalisation parameters were used to normalise the EPI images (Ashburner and Friston, 2005). Spatial smoothing was not done at this step.

2.3.2. Noise filtering

Cardiac and respiratory activity is known to produce signal changes in fMRI time-series (Lund et al., 2006) which could give rise to correlations resembling those observed in rs-fMRI (Birn et al., 2006). In the current study we address these issues by comprehensive filtering of cardiac and respiratory effects (using separate recordings of cardiac and respiratory cycles). Hence, possible confounding effects of residual movement and physiological signals were reduced by filtering several nuisance signals prior to further analysis. The filter was based on a Volterra expansion of the estimated movement parameters obtained from the realignment procedure (24 parameters), a Fourier expansion of the aliased cardiac (10 parameters) and respiratory (6 parameters) cycles and corresponding respiration by cardiac cycle interaction (4 parameters) (Friston et al., 1996; Glover et al., 2000). Also changes in respiration volume over time have shown to produce correlation patterns resembling those observed in rs-fMRI (Birn et al., 2006). To take these changes into account the filter also included 41 delayed versions (from −20 to 20 s) of the respiration volume (Birn et al., 2006). In addition, time-series from white-matter (left and right superior longitudinal fasciculus) and the lateral ventricles were included in the filter. In addition, low frequency scanner drifts were removed by including a discrete cosine basis set with a cut-off frequency of 1/128 Hz.

2.3.3. Regional homogeneity

The regional homogeneity was assessed using the Kendall's Coefficient of Concordance (KCC) measure (also known as Kendall's W). We calculated the KCC for a cube consisting of $3 \times 3 \times 3$ voxels and the KCC-value was assigned to the centre voxel. KCC was calculated as follows: For each voxel each time point was assigned a rank (an integer between 1 and 475) according to signal intensity. The sum of ranks for a given time point i is denoted R_i and the average value of R_i is denoted R_m. The KCC is then calculated as,

$$\mathrm{KCC} = \frac{\sum_{i=1}^{n} (R_i)^2 - n(R_m)^2}{\frac{1}{12}K^2\left(n^3 - n\right)}$$

where $K = 27$ is the number of voxels used in the KCC calculation, and $n = 475$ is the number of time points. The KCC calculation was repeated for each voxel in the brain to create a regional homogeneity map (KCC-map). The KCC-map was then z-transformed by subtracting off the mean KCC of the whole brain and dividing by the standard deviation of all KCC-values in the brain mask (Zuo et al., 2010). When transforming to z-scores, the KCC-map represents values relative to the mean KCC in the brain for each individual subject. KCC-maps were created for each subject using in-house software. Finally, the KCC-maps were smoothed with a $6 \times 6 \times 6$ mm full-width at half maximum Gaussian kernel.

2.3.4. Statistical inference

Since the KCC-maps in general are not guaranteed to be normal distributed, statistical inference at group level employed the non-parametric permutation method using 5000 permutations as implemented in the FSL software tool Randomise (http://fsl.fmrib.ox.ac.uk/fsl/randomise/). We corrected for multiple comparisons by controlling the family-wise error (FWE) rate at the cluster level considering all brain voxels. Cluster extent threshold was set at $p < 0.01$ (two-tailed test) and a corrected p_{FWE}-value < 0.05 at the cluster level was considered statistically significant. Clusters with a corrected p_{FWE}-value < 0.15 are reported as trends. The statistical maps were superimposed on a mean normalised T1-weighted image based on the MPRAGE brain scans of all subjects using Mango (http://ric.uthscsa.edu/mango/). Anatomical locations were inferred using the automated anatomical labeling (AAL) atlas (Tzourio-Mazoyer et al., 2002) for the cerebrum and the probabilistic atlas of the human cerebellum (Diedrichsen et al., 2009) to locate the cerebellar clusters.

We performed two main analyses. The aim of the first analysis was to identify between-group differences in the spatial expression of regional homogeneity including all voxels in the brain. To this end, we compared the KCC-maps of MS patients and healthy controls using a non-parametric two-sample permutation test. The second analysis focused on MS patients exclusively and addressed the question where in the brain regional homogeneity of BOLD-signal fluctuations reflects global disease-related disability. Using only the data of MS patients, we tested for a linear relationship between the voxelwise KCC-values and individual EDSS scores using a non-parametric multiple linear regression model. In both analyses, age was treated as a confounding covariate.

Our main analysis revealed that MS patients show an abnormal expression of regional homogeneity in the cerebellum. This finding motivated a set of explorative post-hoc analyses to gain a deeper pathophysiological understanding of the main results. We performed the same between-group analysis again, but we only included the 34 MS patients who clinically displayed signs of ataxia. We also conducted two exploratory analyses comparing the KCC-maps of patients with ataxia versus patients without ataxia and the KCC-maps of patients with RR-MS versus SP-MS using non-parametric two-sample permutation test with age as covariate. We also tested for a linear relationship between the voxelwise KCC-values and individual ataxia scores in the patient group using a similar multiple regression model with age as covariate.

Since the between-group and regression analyses exclusively revealed changes in the cerebellum, one obvious question was whether the altered regional homogeneity in the cerebellum is related to cerebellar lesion load. We estimated regional lesion load of the cerebellar peduncles because they are the input and output structures of the cerebellum. CST lesion load was also estimated because of its importance for sensory-motor functioning and served as a control tract. Lesion load was extracted for right and left cerebellar peduncles and right and left CST. We tested whether inter-individual variations in lesion load of right and left cerebellar peduncles or right and left CST was linearly correlated with a decrease in mean KCC-values in the right and left cerebellar clusters that had been revealed by the between-group comparison while controlling for the effect of age. In each patient, we extracted the KCC-values from all voxels which belonged to the left cerebellar cluster reaching statistical significance in the between-group comparison. The voxels contributing to the mean KCC of the right cerebellar hemisphere belonged to the cluster showing a trend decrease in KCC in MS relative to healthy controls. The correlations were calculated using Matlab's partial correlation controlling for age. Permutation tests were conducted to assess the significance level (10.000 permutations). The regression analyses were repeated including whole-brain lesion

load as covariate. We tested for a correlation between lesion load of each cerebellar peduncle (i.e., bilateral ROIs for the inferior, middle, and superior peduncle) and the CST (i.e., bilateral ROI including right and left CST) with the mean KCC of the cluster in right and left cerebellum controlling for age.

As a few of the subjects included were left-handed, we repeated the original between-group and regression analysis with EDSS scores using a similar model including both handedness and age as covariates. Finally, we tested whether a shorter resting-state fMRI session would yield the same results as the analysis based on the entire data set recorded over 20 min. This analysis was performed because most resting-state fMRI protocols are shorter. We split the resting-state fMRI data in half and repeated the between-group and the regression analysis with EDSS score on the first half of the resting-state fMRI data (238 volumes). In the additional post-hoc analysis, we applied an uncorrected $p < 0.05$ as statistical threshold.

3. Results

3.1. Reduced regional homogeneity in the cerebellum

Patients with MS showed reduced regional homogeneity in the left cerebellar hemisphere relative to healthy controls ($p_{FWE} = 0.020$; peak Z-score = 4.63; peak coordinate (x,y,z): −18, −46, −26). The area displaying a decrease in regional homogeneity was located in the left superior cerebellar lobe, including mainly lobules V and VI extending into lobule IV and the vermis (Fig. 1). Corresponding regions in the right cerebellar lobule VI with extensions into lobule IV and V showed a similar decrease in regional homogeneity, but reached only trend significance ($p_{FWE} = 0.127$; peak Z-score = 4.21 at voxel (x,y,z): 27, −67, −23). A subcortical cluster comprising right caudate nucleus, thalamus and globus pallidus also reached trend significance ($p_{FWE} = 0.123$; peak Z-score = 4.01 at voxel (x,y,z): 18, 2, 22). In contrast, no area in the hemispheric cortex displayed a significant difference in regional homogeneity in patients with MS relative to healthy controls, even at a more liberal statistical threshold ($p < 0.15$, FWE-corrected). The reduced regional homogeneity in left and right superior cerebellar lobe in MS patients relative to controls could be replicated when removing the patients without ataxia (n = 8) from the analysis ($p_{FWE} = 0.004$; peak Z-score = 4.47 at voxel (x,y,z): 27, −67, −23). The only difference was that the left and right cerebellar clusters merged into one big cluster with the peak voxel localised in the right cerebellar cluster. The main finding, a disease-related reduction in regional homogeneity in patients in the left cerebellar cluster remained significant after including handedness as covariate ($p_{FWE} = 0.022$). The comparison contrasting regional homogeneity in the RR-MS and SP-MS groups yielded no significant differences in regional homogeneity between the phenogroups. Neither were significant differences in regional homogeneity detected between ataxic patients and patients without ataxia. Repeating the main analysis on half of the data, the observed group differences remained significant.

3.2. Relation between regional homogeneity and global clinical disability

Regression analysis identified a single cluster in the left cerebellar posterior lobe where regional homogeneity decreased with increasing clinical disability as expressed by the EDSS score. The more the MS patients were clinically affected (i.e. the higher the individual EDSS score), the weaker was regional homogeneity in the left cerebellar cluster (Fig. 2; $p_{FWE} = 0.031$; peak Z-score = 4.52 at voxel (x,y,z): −21, −82, −32). The cerebellar cluster covered Crus I and extended into Crus II and the left dentate nucleus. A homologous area in the right cerebellum comprising Crus I and parts of Crus II showed a similar relationship between regional homogeneity and individual EDSS scores, but this trend did not reach statistical significance ($p_{FWE} = 0.096$; peak Z-score = 3.98 at voxel (x,y,z): 27, −70, −38). The observed inverse linear relationship between KCC-values and EDSS scores remained significant after including handedness as covariate ($p_{FWE} = 0.033$). A regression analysis that only used the first half of the resting-state fMRI data replicated the linear relation between EDSS score and KCC in the left cerebellar cluster. Additionally, the right cerebellar cluster became significant that failed to reach significance in the original analysis using the entire fMRI data set.

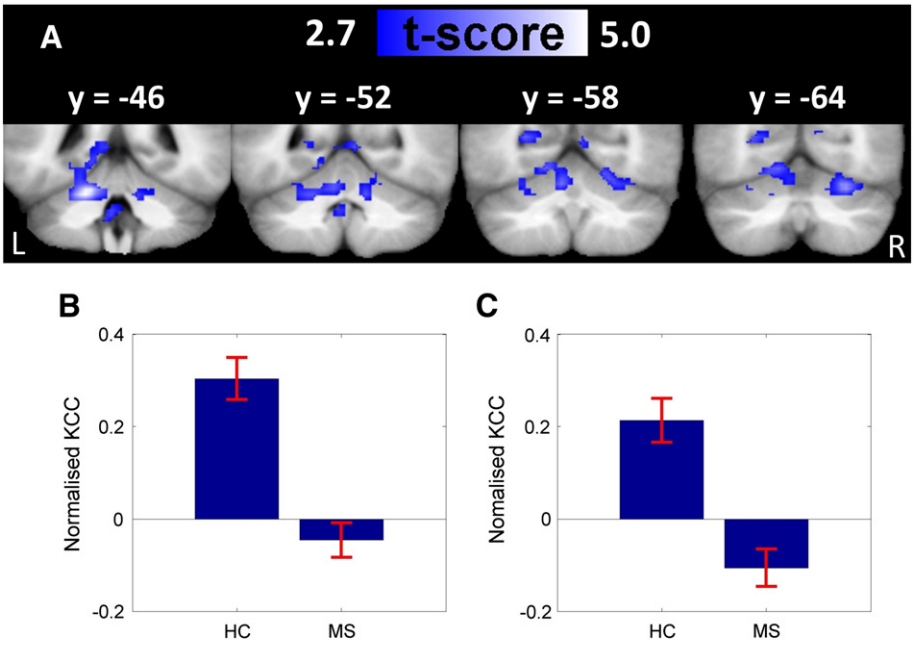

Fig. 1. Decrease in regional homogeneity of cerebellar regions in MS. Coronal t-maps representing voxels with reduced regional homogeneity in MS compared with controls (A). Left (B) and right (C) cerebellar cluster mean normalised KCC and standard error bars of healthy controls and MS patients. KCC = Kendall's Coefficient of Concordance; HC = healthy controls; MS = multiple sclerosis.

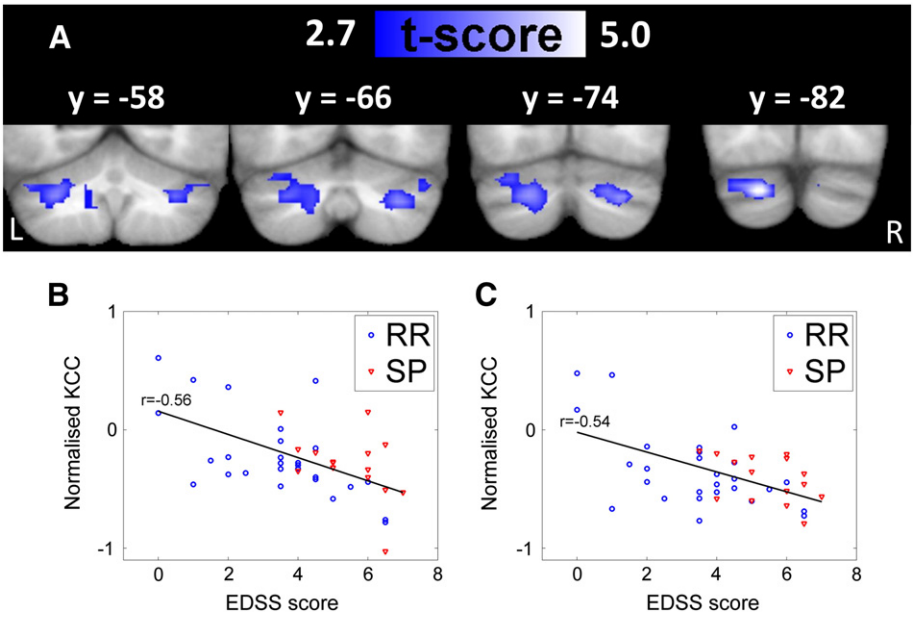

Fig. 2. Regional homogeneity of cerebellar regions correlates with disability in MS. Coronal t-maps representing voxels where KCC correlated with EDSS scores in MS (A). Left (B) and right (C) cerebellar cluster mean normalised KCC for each subject (y-axis) plotted against EDSS scores (x-axis) with a regression line. KCC = Kendall's Coefficient of Concordance; EDSS = Expanded Disability Status Scale; RR = relapsing–remitting multiple sclerosis; SP = secondary progressive multiple sclerosis.

Exploratory post-hoc regression analysis identified a single brain cluster in the left cerebellar posterior lobe where regional homogeneity decreased with increasing ataxia scores (Fig. 3; $p_{FWE} = 0.047$; peak Z-score = 3.61 at voxel (x,y,z): −6, −52, −41). This cluster also comprised Crus II and Crus I, extending into the left dentate nucleus and lobule IX. The cluster showing reductions in regional homogeneity with increasing EDSS scores showed only limited overlap (20% of voxels) with the cluster displaying decreases in regional homogeneity with increasing ataxia scores (Fig. 3), although individual ataxia and EDSS scores were highly correlated (correlation coefficient = 0.68; $p < 0.001$).

3.3. Relation between regional homogeneity and lesion load in the cerebellum

In the 41 patients in whom structural MRI data of sufficient quality were available lesion load of the cerebellar peduncles and CST were extracted. The volume of the right cerebellar peduncle template was estimated to 9.6 ml and the volume of left cerebellar peduncle template 9.9 ml. The maximal lesion load of the cerebellar peduncles accounted for 1.1 ml, corresponding to 5.9% of the total cerebellar peduncles volume (Table 1).

The correlations between cerebellar regional homogeneity and lesion load of the cerebellar peduncles and CST are illustrated in Fig. 4. Lesion load of the left cerebellar peduncle showed a significant partial correlation with the regional mean KCC in the left ($p = 0.005$) and right cerebellum ($p = 0.016$), whereas lesion load of right cerebellar peduncles showed no significant linear relation with right or left cerebellar regional mean KCC ($p \geq 0.097$). The results were reproduced when repeating the regression analyses controlling for whole-brain lesion load. We also segregated lesion load of the bilateral superior, middle, and inferior cerebellar peduncles and correlated these lesion measures with left and right cerebellar regional mean KCC. Lesion load of middle cerebellar peduncles showed a significant partial correlation with left ($p = 0.012$) and right cerebellar regional mean KCC ($p = 0.042$). Lesion load of inferior cerebellar peduncles showed a significant partial correlation with left regional mean KCC ($p = 0.029$), and lesion load of superior cerebellar peduncle showed a trend towards a partial correlation with right cerebellar regional mean KCC ($p = 0.072$). Lesion load in left, right or bilateral CST showed no linear correlation with right or left cerebellar regional mean KCC ($p > 0.2$). The overall lesion load of the right ($p = 0.012$) and left ($p = 0.044$) cerebellar peduncles showed a significant positive relationship with individual EDSS scores.

4. Discussion

Using regional homogeneity of resting-state fluctuations in the BOLD-signal as index of local functional connectivity, we show that local functional connectivity is impaired in the left cerebellum in MS. Regional homogeneity was found to be reduced in lobules V and VI of the left cerebellar hemisphere in patients with MS relative to controls. Further, patients with higher EDSS scores displayed less local connectivity in Crus I and dentate nucleus of left cerebellum. Similar trends were present in homologous regions of the right cerebellum. Post-hoc analyses showed that patients with higher lesion load of the left cerebellar peduncle showed more reduced local cerebellar connectivity.

4.1. Cerebellar regional homogeneity in MS

The impairment of regional functional homogeneity in MS extends previous reports showing marked pathological changes in cerebellar

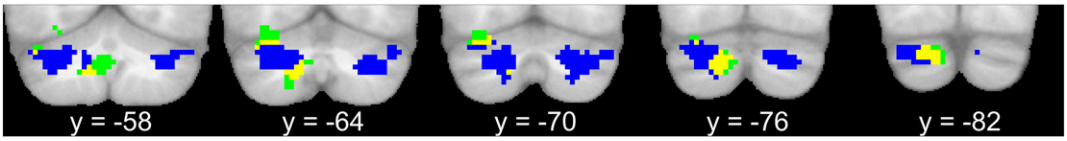

Fig. 3. Regional homogeneity of cerebellar regions correlates with ataxia in MS. Coronal maps representing voxels where KCC correlated with individual ataxia scores in MS (green cluster). The blue cluster represents voxels where KCC correlated with EDSS scores in MS. The significant clusters of the two analyses showed limited spatial overlap (20% of voxels; yellow cluster represented in the foreground) and mainly include Crus I (40%), Crus II (14%), the dentate nucleus (9%), lobule IX (9%), and lobule VI (10%).

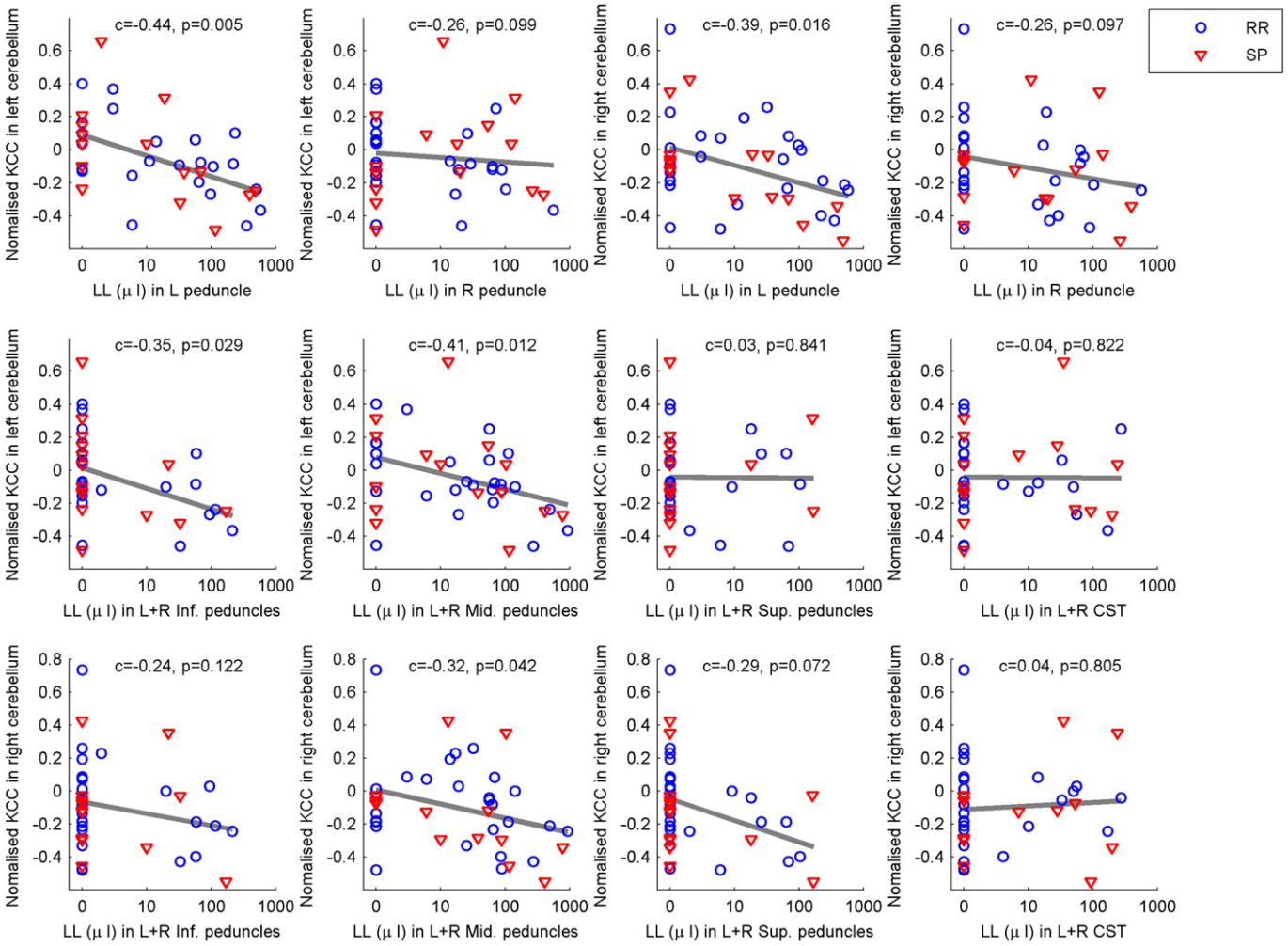

Fig. 4. Correlation between cerebellar regional homogeneity and lesion load of the cerebellar peduncles and cortico-spinal tract. The first row illustrates the correlations between regional homogeneity in left or right cerebellar region-of-interest (ROI) with lesion load of left or right cerebellar peduncles. The second row illustrates the correlations between regional homogeneity of the left cerebellar ROI and lesion load of the bilateral inferior, middle, and superior cerebellar peduncles and cortico-spinal tract (CST). The third row illustrates the correlations between regional homogeneity of the right cerebellar ROI and lesion load of the bilateral inferior, middle, and superior cerebellar peduncles and CST. KCC = Kendall's Coefficient of Concordance; LL = lesion load; L = left; R = right; RR = relapsing–remitting MS; SP = secondary progressive MS; CST = cortico-spinal tract; Inf. peduncles = inferior cerebellar peduncles; Mid. peduncles = middle cerebellar peduncles; Sup. peduncles = superior cerebellar peduncles.

cortex in MS (Anderson et al., 2009; Gilmore et al., 2009; Kutzelnigg et al., 2007). The cerebellum is critically involved in the temporal and spatial integration of neural inputs from both descending cortical afferents (cortico-ponto-cerebellar projections) and ascending spinal afferents (proprioceptive information via spino-cerebellar projections) via the cerebellar peduncles (Ramnani, 2006). The reduced cerebellar regional homogeneity might indicate that the temporo-spatial integration of converging cortico-ponto-cerebellar and spino-cerebellar inputs is disintegrated in patients with MS. The notion of dysfunctional neural integration in the cerebellum is supported by a series of positron emission tomography studies which found bilateral reductions in cerebellar resting-state glucose metabolism in early RR-MS which was ascribed to the remote effect of demyelinating lesions (i.e. crossed cerebellar diaschisis) (Blinkenberg et al., 2000; Derache et al., 2006). In addition, two activation fMRI studies have reported decreased inter-regional functional and effective connectivity during motor task involving cerebellar regions in MS (Rocca et al., 2009; Saini et al., 2004).

Disrupted local connectivity in the cerebellum might be caused primarily by local cortical damage. Alternatively, MS lesions in cerebellar white-matter tracts might cause a functional disruption of neurotransmission in these pathways. The latter hypothesis is supported by the finding that patients displayed more reduced right and left cerebellar regional homogeneity with increasing lesion load of the left cerebellar peduncle. In particular, lesion load in the middle cerebellar peduncle correlated with the decrease in regional cerebellar connectivity. The middle cerebellar peduncle is a main input structure containing axons which project from the nuclei pontis of the opposite side to the cerebellar cortex. This structure–function relationship suggests that the disturbed regional integration of incoming cortico- and spino-cerebellar information increases with lesion load in the cerebellar peduncles, but this hypothesis needs to be tested specifically in future studies.

When interpreting the present results, one needs to take into account the neuroanatomical organisation of the cerebellum. Research has provided converging evidence that Crus I and Crus II represent the 'cognitive' cerebellum and lobules V–VI primarily represent the sensory-motor cerebellum (Kelly and Strick, 2003; Krienen and Buckner, 2009; O'Reilly et al., 2010). The between-group difference in regional homogeneity was located in motor territories of the cerebellar hemisphere, namely the cerebellar lobules V and VI that are connected with cortical motor regions. Motor impairment is prevalent in MS and is mainly caused by lesions located along the CST, in particular in the spinal cord. However, we found no relation between regional homogeneity of the cerebellum and CST lesion load. This negative finding has, however, to be interpreted with caution because our scanning protocol did not cover the spinal cord where local lesions significantly contribute to motor disability.

4.2. Local resting-state connectivity and clinical disability

Regional homogeneity of resting-state BOLD-signal fluctuations in the cerebellum correlated negatively with clinical disability as reflected by the EDSS score. Surprisingly, it was in cognitive (e.g. Crus I and Crus II) rather than motor territories of the cerebellum where the decrease in local functional connectivity was more pronounced in patients with higher disability scores. We attribute this preferential association between disease-related disability and reduced regional connectivity in cognitive areas of the cerebellar cortex to the 'resting-state' during which the fMRI data were recorded. The 'resting-state' represents a more introspective state in which cognitive operations like day-dreaming take place (Mason et al., 2007), while the motor system is idling. In fact, specifically Crus I has shown to be functionally connected with a network of cortical regions similar to the default-mode network (Krienen and Buckner, 2009) which is a network associated with introspection, remembering the past and planning the future (Buckner and Vincent, 2007). If this explanation were correct, an association between a reduction in regional functional connectivity in the motor cerebellum and disease-related disability might become more obvious during a task requiring sustained motor activity (e.g. tonic contraction or tapping movements).

A negative linear relationship was also found between regional homogeneity and the amount of ataxia: The stronger ataxia, the lower was local resting-state connectivity in the cerebellum. Ataxia was a frequent symptom in the patient group. 80% of the patients suffered from ataxia which is in good agreement with the relative frequency of ataxia reported in the literature (Kurtzke, 1970; Swingler and Compston, 1992). Since the EDSS also includes the assessment of cerebellar dysfunction, it is not surprising that the ataxia and EDSS scores were highly correlated. Despite of the tight relationship between these two clinical measures, the cerebellar cluster showing a correlation between reduced local resting-state connectivity and ataxia showed little spatial overlap with the cluster showing a correlation between local resting-state connectivity and EDSS. This raises the possibility that certain 'symptom clusters' might be associated with different spatial patterns of disrupted local resting-state connectivity in the cerebellum. This possibility remains to be examined more systematically in future studies.

The left cerebellar cluster showing a stronger decrease in local connectivity with increasing disability extended into the dentate nucleus. From a circuit perspective, the dentate nucleus is located downstream to the cerebellar cortex receiving its input from the Purkinje cells. Given that the dentate nucleus is the major cerebellar output channel projecting to primary motor, premotor, oculomotor, prefrontal, and posterior parietal areas of the cortex via synapses in the thalamus and basal ganglia (Dum and Strick, 2003; Hoshi et al., 2005), the dentate nucleus is in a particularly strategic position to transmit the negative consequences of aberrant cerebellar processing to the neocortical networks. This might explain why disrupted regional integration in the dentate nucleus was significantly related to clinical disability. An additional link between an alteration of the dentate nucleus and clinical disability has recently been reported in a structural MRI study which focused on regional T2* hypointensities suggestive of pathologic iron deposition in MS (Tjoa et al., 2005). Regional T2* hypointensity in dentate nucleus was found to be the only variable that correlated with ambulatory impairment and the EDSS score.

4.3. Local versus long-range network connectivity

Outside the cerebellum, no brain region showed a significant alteration in regional homogeneity or a correlation between regional homogeneity and clinical disability. By applying a whole-brain network analysis to the same rs-fMRI data set, we have previously shown that several subcortical clusters in the cerebral hemisphere located in the thalamus and basal ganglia have a stronger long-range connectivity with the motor resting-state network in the same group of MS patients (Dogonowski et al., 2012). This up-regulation of motor long-range motor connectivity in the basal ganglia and thalamus as revealed by the whole-brain network analysis was not accompanied by alterations in local functional connectivity. Likewise, the changes in local resting-state connectivity in the motor part of the cerebellum were not associated with alterations in long-range motor resting-state connectivity. Together, the complementary analyses of resting-state functional connectivity prompt two conclusions. From a methodological point, it can be concluded that alterations in long-range and local resting-state connectivity are not two sides of the same coin, and therefore can well dissociate. While long-range connectivity reflects communication between distinct network nodes, local resting-state connectivity do tell something about how fine grained local neural activity is temporo-spatially correlated within a network node.

With respect to the pathophysiology of multiple sclerosis, the data indicate that cerebral subcortical structures and the cerebellum show different alterations in resting-state connectivity: While the basal ganglia and thalamus show an expanded long-range motor connectivity, changes in local functional connectivity seem to prevail in the cerebellum. This study suggests a possible link between lesion load of the cerebellar peduncles and changes in local connectivity taking place in the cerebellum. The lesioned cerebellar peduncles in MS might become a bottleneck causing deficient parallel information transfer into the cerebellum reflected by a reduction in cerebellar local functional connectivity. The more expanded long-range connectivity of the basal ganglia and thalamus might be indicative of an impaired funnelling function of the basal ganglia and thalamus secondary to a scattered disruption of cortico-thalamic and cortico-striatal inputs due to hemispheric lesions (Dogonowski et al., 2012).

4.4. Methodological considerations

In this study, we used a relatively long rs-fMRI session collecting a comprehensive resting-state data set containing 480 volumes (20 min. acquisition) for each subject. However, we were able to reproduce the main results when only using the first half of the resting-state fMRI data (i.e., the first 238 volumes of a single session). This suggests that the sensitivity of the rs-fMRI approach might not necessarily increase when raising the number of samples in a session. Especially with respect to the long recording time, it might have been preferable to record resting-state fMRI with the subjects having the eyes open and monitoring of eye movements and electroencephalographic activity to capture any reduction in vigilance. Another limitation of this study is that no cognitive tests were performed. This prevented us from relating local connectivity changes in the 'cognitive' cerebellum to cognitive impairments. The local connectivity changes in the right cerebellum only reached trend significance. A larger sample size might have increased the chance to yield significant changes in local connectivity also in the right cerebellum. The cross-sectional study design also has some inherent limitations. Better insights into the dynamics of functional brain connectivity changes in MS are expected from longitudinal resting-state fMRI studies which allow to trace the dynamic expression of impaired local and long-range resting-state connectivity during the course of MS and to relate these to the dynamics of clinical impairment.

We were able to relate cerebellar reductions in local connectivity with lesion load of the cerebellar peduncles. In future studies, it would be interesting to estimate the radial extension of each T2-weighted lesion perpendicular to the peduncle axis or to test impairment of anatomical connectivity in the peduncles with diffusion MRI. This would give a better picture of the extent of impairment of the input and output structures of the cerebellum and might help to establish a more causal link between structural damage of the cerebellar peduncles and local changes in cerebellar resting-state connectivity.

Funding

This work was supported by the Danish Multiple Sclerosis Society (R110-A3506, R192-A10127); intramural research grant of Hvidovre

Hospital; and a partial Ph.D. stipend from the University of Copenhagen, Faculty of Health Sciences. Hartwig R. Siebner was supported by a Grant of Excellence sponsored by The Lundbeck Foundation *Mapping, Modulation & Modeling the Control of Actions (ContAct)* (R59-A5399). The MR scanner was donated by the Simon Spies Foundation.

Competing interests

A-M. Dogonowski has received speaker's fee from Biogen Idec and Merck-Serono. Congress fee to ECTRIMS 2010 was covered by Merck-Serono. **K. Winther Andersen** reports no disclosures. **K.H. Madsen** reports no disclosures**. P. Soelberg Sørensen** has served on scientific advisory boards Biogen Idec, Merck-Serono, Novartis, Genmab, TEVA, Elan, GSK, has been on steering committees or independent data monitoring boards in clinical trials sponsored by Merck-Serono, Genmab, TEVA, GSK, Bayer Schering, and he has received funding of travel for these activities; has served as Editor-in-Chief of the European Journal of Neurology, and is currently editorial board member for Multiple Sclerosis Journal, European Journal of Neurology, Therapeutic Advances in Neurological Disorders and; has received speaker honoraria from Biogen Idec, Merck-Serono, TEVA, Bayer Schering, Sanofi-Aventis, Genzyme, and Novartis; and has received payment for writing and reviewing manuscript from IBI Consulting, a division of Informa plc. His department has received research support from Biogen Idec, Bayer Schering, Merck-Serono, TEVA, Baxter, Sanofi-Aventis, BioMS, Novartis, Bayer, RoFAR, Roche, Genzyme, from the Danish Multiple Sclerosis Society, the Danish Medical Research Council, and the European Union Sixth Framework Programme: Life sciences, Genomics and Biotechnology for health. **O.B. Paulson** has served on the scientific advisory board of 7 T MR Tomographie/Hochfeld MR Zentrum, Wien, Austria; is member of the Swedish 7 T MR steering group; is member of the board of directors of the Elsass foundation; is counsellor for the Danish Governmental Department of Justice in medico legal aspects; has received grants from the Lundbeck foundation; has received a speaker's fee from BK Medical, Herlev, Denmark. **M. Blinkenberg** has served on scientific advisory boards for Biogen Idec, Merck-Serono, Novartis, Sanofi-Aventis and Teva; has received speaker honoraria from Biogen Idec, Merck-Serono, Bayer-Schering, Novartis, Teva and Sanofi-Aventis; has received consulting honoraria from the Danish Multiple Sclerosis Society, Biogen Idec and Merck-Serono; has received funding for travel from Biogen Idec, Merck-Serono, Sanofi-Aventis, Genzyme and Solvay Pharma; has received research support from Merck-Serono and the Danish Multiple Sclerosis Society. **H.R. Siebner** serves as a member on a scientific advisory board for Lundbeck A/S, Valby, Denmark (2012) and as handling editor of Neuroimage; has received royalties from Springer Publishing for a textbook on transcranial magnetic stimulation (published in german, 2007–2010); has received speaker honorarium from Biogen Idec Denmark A/S (2012); had received research support for: Mapping brain reorganisation of higher visual and multisensory perception in sighted and blind individuals with magnetic resonance imaging and transcranial brain stimulation, Forsknings-og Innovationsstyrelsen, Grant Nr. 09-075595; Mapping maladaptive motor connectivity underlying peak-of-dose dyskinesia in Parkinson disease: a functional MRI study, Forskningsrådet for Sundhed og Sygdom Forsknings- og Innovationsstyrelsen—Danmark, grant nr. 09-072163; Mapping brain reorganisation of higher visual and multisensory perception in sighted and blind individuals, Forsknings- og Innovationsstyrelsen Danmark, Int. Netværks-aktivitet med Israel, grant nr. 09-075595. Support from a non-profit foundation or society: Vurdering af eksperimentelle skizofreni modeller med MR billeddannelse—relevans i forhold til klinikken, Savværksejer Jeppe Juhls og hustru Ovita Juhls Mindelegat 2010; Integration of cortical information in the human striatum: non-invasive assessment with magnetic resonance imaging. LundbeckFonden, grant nr. R48 A4846; Structural grant to establish a 7 T MRI facility, The John and Birthe Meyer Foundation (no grant nr.); Identifying changes in whole-brain functional connectivity in multiple sclerosis using resting-state functional MRI, Scleroseforeningen Denmark, grant nr. R192-A10127; Mapping, Modulation & Modeling the Control of Actions (ContAct). LundbeckFonden. Grant nr. R59 A5399.

Acknowledgements

We wish to thank the participants. We thank Dr. Per Åkeson for radiological advice on accidental structural brain findings.

References

Anderson, V.M., Fisniku, L.K., Thompson, A.J., Miller, D.H., Altmann, D., 2009. MRI measures show significant cerebellar gray matter volume loss in multiple sclerosis and are associated with cerebellar dysfunction. Mult. Scler. 15, 811–817.
Ashburner, J., Friston, K.J., 2005. Unified segmentation. Neuroimage 26, 839–851.
Birn, R.M., Diamond, J.B., Smith, M.A., Bandettini, P.A., 2006. Separating respiratory-variation-related fluctuations from neuronal-activity-related fluctuations in fMRI. Neuroimage 31, 1536–1548.
Blinkenberg, M., Rune, K., Jensen, C.V., Ravnborg, M., Kyllingsbæk, S., Holm, S., Paulson, O., Sørensen, P., 2000. Cortical cerebral metabolism correlates with MRI lesion load and cognitive dysfunction in MS. Neurology 54, 558–564.
Buckner, R.L., Vincent, J.L., 2007. Unrest at rest: default activity and spontaneous network correlations. Neuroimage 37, 1091–1096.
Derache, N., Marié, R.-M., Constans, J.-M., Defer, G.-L., 2006. Reduced thalamic and cerebellar rest metabolism in relapsing–remitting multiple sclerosis, a positron emission tomography study: correlations to lesion load. J. Neurol. Sci. 245, 103–109.
Diedrichsen, J., Balsters, J.H., Flavell, J., Cussans, E., Ramnani, N., 2009. A probabilistic MR atlas of the human cerebellum. Neuroimage 46, 39–46.
Dogonowski, A.-M., Siebner, H.R., Soelberg, P., Wu, X., Biswal, B., Paulson, O.B., Dyrby, T.B., Skimminge, A., Blinkenberg, M., Madsen, K.H., 2012. Expanded functional coupling of subcortical nuclei with the motor resting-state network in multiple sclerosis. Mult. Scler. 19, 559–566.
Dum, R.P., Strick, P.L., 2003. An unfolded map of the cerebellar dentate nucleus and its projections to the cerebral cortex. J. Neurophysiol. 89, 634–639.
Friston, K.J., Williams, S., Howard, R., Frackowiak, R.S., Turner, R., 1996. Movement-related effects in fMRI time-series. Magn. Reson. Med. 35, 346–355.
Gilmore, C.P., Donaldson, I., Bö, L., Owens, T., Lowe, J., Evangelou, N., 2009. Regional variations in the extent and pattern of grey matter demyelination in multiple sclerosis: a comparison between the cerebral cortex, cerebellar cortex, deep grey matter nuclei and the spinal cord. J. Neurol. Neurosurg. Psychiatry 80, 182–187.
Glover, G.H., Li, T.Q., Ress, D., 2000. Image-based method for retrospective correction of physiological motion effects in fMRI: RETROICOR. Magn. Reson. Med. 44, 162–167.
Hawellek, D.J., Hipp, J.F., Lewis, C.M., Corbetta, M., Engel, A.K., 2011. Increased functional connectivity indicates the severity of cognitive impairment in multiple sclerosis. Proc. Natl. Acad. Sci. U. S. A. 108, 19066–19071.
He, Y., Wang, L., Zang, Y., Tian, L., Zhang, X., Li, K., Jiang, T., 2007. Regional coherence changes in the early stages of Alzheimer's disease: a combined structural and resting-state functional MRI study. Neuroimage 35, 488–500.
Hoshi, E., Tremblay, L., Féger, J., Carras, P.L., Strick, P.L., 2005. The cerebellum communicates with the basal ganglia. Nat. Neurosci. 8, 1491–1493.
Hua, K., Zhang, J., Wakana, S., Jiang, H., Li, X., Reich, D.S., Calabresi, P.A., Pekar, J.J., van Zijl, P.C., Mori, S., 2008. Tract probability maps in stereotaxic spaces: analyses of white matter anatomy and tract-specific quantification. NeuroImage 39, 336–347.
Kelly, R.M., Strick, P.L., 2003. Cerebellar loops with motor cortex and prefrontal cortex of a nonhuman primate. J. Neurosci. 23, 8432–8444.
Krienen, F.M., Buckner, R.L., 2009. Segregated fronto-cerebellar circuits revealed by intrinsic functional connectivity. Cereb. Cortex 19, 2485–2497.
Kurtzke, J.F., 1970. Clinical manifestations of multiple scleorsis. In: Vinken, P.J., Bruyn, G.W. (Eds.), Handbook of Clinical Neurology, Amsterdam, pp. 161–216.
Kurtzke, J.F., 1983. Rating neurologic impairment in multiple sclerosis: an expanded disability status scale (EDSS). Neurology 33, 1444–1452.
Kutzelnigg, A., Faber-Rod, J.C., Bauer, J., Lucchinetti, C.F., Sorensen, P.S., Laursen, H., Stadelmann, C., Brück, W., Rauschka, H., Schmidbauer, M., Lassmann, H., 2007. Widespread demyelination in the cerebellar cortex in multiple sclerosis. Brain Pathol. 17, 38–44.
Liang, P., Liu, Y., Jia, X., Duan, Y., Yu, C., Qin, W., Dong, H., Ye, J., Li, K., 2011. Regional homogeneity changes in patients with neuromyelitis optica revealed by resting-state functional MRI. Clin. Neurophysiol. 122, 121–127.
Lowe, M.J., Phillips, M.D., Lurito, J.T., Mattson, D., Dzemidzic, M., Mathews, V.P., 2002. Multiple sclerosis: low-frequency temporal blood oxygen level-dependent fluctuations indicate reduced functional connectivity initial results. Radiology 224, 184–192.
Lund, T.E., Madsen, K.H., Sidaros, K., Luo, W., Nichols, T.E., 2006. Non-white noise in fMRI: does modelling have an impact? Neuroimage 29, 54–66.
Mason, M.F., Norton, M.I., Van Horn, J.D., Wegner, D.M., Grafton, S.T., Macrae, C.N., 2007. Wandering minds: the default network and stimulus-independent thought. Science 315, 393–395.
O'Reilly, J.X., Beckmann, C.F., Tomassini, V., Ramnani, N., Johansen-Berg, H., 2010. Distinct and overlapping functional zones in the cerebellum defined by resting state functional connectivity. Cereb. Cortex 20, 953–965.
Oldfield, R.C., 1971. Assessment and analysis of handedness—Edinburgh inventory. Neuropsychologia 9, 97–113.
Polman, C.H., Reingold, S.C., Edan, G., Filippi, M., Hartung, H.P., Kappos, L., Lublin, F.D., Metz, L.M., McFarland, H.F., O'Connor, P.W., Sandberg-Wollheim, M., Thompson, A.J.,

Weinshenker, B.G., Wolinsky, J.S., 2005. Diagnostic criteria for multiple sclerosis: 2005 revisions to the "McDonald Criteria". Ann. Neurol. 58, 840–846.
Ramnani, N., 2006. The primate cortico-cerebellar system: anatomy and function. Nat. Rev. Neurosci. 7, 511–522.
Ravnborg, M., Grønbech-Jensen, M., Jønsson, A., 1997. The MS Impairment Scale: a pragmatic approach to the assessment of impairment in patients with multiple sclerosis. Mult. Scler. 3, 31–42.
Rocca, M.A., Absinta, M., Valsasina, P., Ciccarelli, O., Marino, S., Rovira, A., Gass, A., Wegner, C., Enzinger, C., Korteweg, T., 2009. Abnormal connectivity of the sensorimotor network in patients with MS: a multicenter fMRI study. Hum. Brain Mapp. 30, 2412–2425.
Rocca, M.A., Valsasina, P., Absinta, M., Riccitelli, G., Rodegher, M.E., Misci, P., Rossi, P., Falini, A., Comi, G., Filippi, M., 2010. Default-mode network dysfunction and cognitive impairment in progressive MS. Neurology 74, 1252–1259.
Roosendaal, S.D., Schoonheim, M.M., Hulst, H.E., Sanz-Arigita, E.J., Smith, S.M., Geurts, J.J.G., Barkhof, F., 2010. Resting state networks change in clinically isolated syndrome. Brain 133, 1612–1621.
Saini, S., DeStefano, N., Smith, S., Guidi, L., Amato, M.P., Federico, A., Matthews, P.M., 2004. Altered cerebellar functional connectivity mediates potential adaptive plasticity in patients with multiple sclerosis. J. Neurol. Neurosurg. Psychiatry 75, 840–846.
Swingler, R.J., Compston, D.A., 1992. The morbidity of multiple sclerosis. Q. J. Med. 83, 325–337.
Tjoa, C.W., Benedict, R.H.B., Weinstock-Guttman, B., Fabiano, A.J., Bakshi, R., 2005. MRI T2 hypointensity of the dentate nucleus is related to ambulatory impairment in multiple sclerosis. J. Neurol. Sci. 234, 17–24.
Trapp, B.D., Peterson, J., Ransohoff, R.M., Rudick, R., Mörk, S., Bö, L., 1998. Axonal transection in the lesions of multiple sclerosis. N. Engl. J. Med. 338, 278–285.
Tzourio-Mazoyer, N., Landeau, B., Papathanassiou, D., Crivello, F., Etard, O., Delcroix, N., Mazoyer, B., Joliot, M., 2002. Automated anatomical labeling of activations in SPM using a macroscopic anatomical parcellation of the MNI MRI single-subject brain. Neuroimage 15, 273–289.
Wu, T., Long, X., Zang, Y., Wang, L., Hallett, M., Li, K., Chan, P., 2009. Regional homogeneity changes in patients with Parkinson's disease. Hum. Brain Mapp. 30, 1502–1510.
Zang, Y., Jiang, T., Lu, Y., He, Y., Tian, L., 2004. Regional homogeneity approach to fMRI data analysis. Neuroimage 22, 394–400.
Zuo, X.N., Di Martino, A., Kelly, C., Shehzad, Z.E., Gee, D.G., Klein, D.F., Castellanos, F.X., Biswal, B.B., Milham, M.P., 2010. The oscillating brain: complex and reliable. Neuroimage 49, 1432–1445.